Acta Oceanol. Sin., 2017, Vol. 36, No. 6, P. 34–46
DOI: 10.1007/s13131-017-1004-4
http://www.hyxb.org.cn
E-mail: hyxbe@263.net

The effect of Fe-Mn minerals and seawater interface and enrichment mechanism of ore-forming elements of polymetallic crusts and nodules from the South China Sea

GUAN Yao[1, 2], SUN Xiaoming[1, 2, 3, 4]*, JIANG Xiaodong[3], SA Rina[3], ZHOU Li[1, 2], HUANG Yi[3], LIU Yating[1, 2], LI Xiaojie[1, 2], LU Rongfei[1, 2], WANG Chi[1, 2]

[1] School of Marine Sciences, Sun Yat-sen University, Guangzhou 510006, China

[2] Guangdong Provincial Key Laboratory of Marine Resources and Coastal Engineering, Guangzhou 510006, China

[3] School of Earth Sciences and Geological Engineering, Sun Yat-sen University, Guangzhou 510275, China

[4] State Key Laboratory for Mineral Deposits Research, Nanjing University, Nanjing 210046, China

Received 16 February 2016; accepted 18 April 2016

Abstract

Ferromanganese crusts and nodules are important submarine mineral resources that contain various metal elements with significant economic value. In this study, polymetallic crusts and nodules obtained from the South China Sea (SCS) were determined by using X-ray power diffraction (XRD), Raman spectroscopy (RS), Fourier transform infrared spectroscopy (FTIR), and X-ray photoelectron spectroscopy (XPS) to systematically investigate and analyze the mineralogical and spectral characteristics of the Fe-Mn minerals. XRD measurements revealed that the SCS polymetallic crusts and nodules were composed of vernadite, quartz, and plagioclase. The nodules also contained todorokite. The Fe-phase minerals of the SCS crusts and nodules were composed of amorphous Fe oxide/hydroxide, and the Mn- and Fe-phases minerals exhibited relatively poor degrees of crystallization. FTIR results showed that the Fe-Mn minerals in the crusts and nodules included a large number of surface hydroxyl groups. These surface hydroxyl groups contained protons that could provide reactive sites for complexation of ore-forming elements in seawater. XPS results indicated that the surfaces of the Fe-Mn minerals mainly contained Fe, Mn, and O. Fe was present in the trivalent oxidation state, while Mn, which may contain several bivalent oxidation state, was present in the tetravalent and trivalent oxidation states. The SCS polymetallic crusts and nodules were compared with Pacific seamount crusts, and results showed that the surface hydroxyl (-OH) groups of the SCS crusts and nodules numbered more than the lattice oxygen (O^{2-}). But the lattice oxygen of Pacific seamount crusts numbered more than the surface hydroxyl groups. This characteristic indicated that the degree of crystallization of Fe-Mn minerals from the Pacific Ocean was higher than that of minerals from the South China Sea. Comprehensive studies showed that ore-forming elements in the interface between seawater and the Fe-Mn minerals in the submarine ferromanganese crusts and nodules employed the following enrichment mechanisms: (1) the metal ion complexed with the surface hydroxyl of Fe-Mn minerals to form hydroxyl complexes, which were connected by coordination bonds or stable inner-sphere complexes that exchanged protons on the mineral surfaces; (2) the charged surfaces of the minerals and metal cations formed outer-sphere complexes, which made up the electrostatic double layer, through electrostatic adsorption; and (3) the metal cations isomorphously exchanged the Mn and Fe ions of the mineral lattice structure.

Key words: polymetallic crust and nodule, mineralogy characteristic, interface effect, element enrichment, surface complexation

Citation: Guan Yao, Sun Xiaoming, Jiang Xiaodong, Sa Rina, Zhou Li, Huang Yi, Liu Yating, Li Xiaojie, Lu Rongfei, Wang Chi. 2017. The effect of Fe-Mn minerals and seawater interface and enrichment mechanism of ore-forming elements of polymetallic crusts and nodules from the South China Sea. Acta Oceanologica Sinica, 36(6): 34–46, doi: 10.1007/s13131-017-1004-4

1 Introduction

Seafloor ferromanganese crusts and nodules are important mineral resources. These seafloor features are concentrated with an abundance of metal elements, such as Mn, Co, Cu, Ni, Mo, Te, rare earth elements (REE), and platinum group elements (PGE). China, along with many other countries has investigated the seabed ferromanganese crusts and nodules of the world's oceans (He et al., 2011a), and the genesis of these sea features has been extensively discussed (Xue, 2007; He et al., 2011b; Hein and Koschinsky, 2014; Hein et al., 2015; Guan et al., 2017). While the

Foundation item: The National Natural Science Foundation of China under contract Nos 40473024 and 40343019; the research fund from State Key Laboratory for Mineral Deposits Research in Nanjing University under contract No. 20-15-07; the Investigation and Development of Marine Resources during the 12th Five Year Plan Project under contract No. DY125-13-R-05; the Doctoral Program of Higher Education Research Fund under contract Nos 20040558049 and 20120171130005; the Project of High Level Talents in Colleges of Guangdong Province (2011) and the Fundamental Research Funds for Central Universities under contract Nos 16lgjc11, 12lgjc05 and 09lgpy09.

*Corresponding author, E-mail: eessxm@mail.sysu.edu.cn

pronounced degree of enrichment of ore-forming elements in seafloor crusts and nodules is of great interest, the enrichment mechanism of these elements in ferromanganese crusts and nodules has not yet been well elucidated. Hein et al. (2000) and Kuhn et al. (1998) suggested that the obvious enrichment of some trace elements in hydrogenetic ferromanganese minerals is related to their slow growth rates, thereby implying a time-dependent enrichment process. Several studies have indicated that the enrichment of many redox-sensitive metals is due to redox reactions occurring through uptake of Fe-Mn mineral phases during their formation. Surface oxidation during adsorption on the Fe-Mn mineral phases has been suggested for Pt (Halbach et al., 1989), and the pronounced enrichment of Te in the ferromanganese crusts and nodules has been explained by the surface oxidation mechanism (Hein et al., 2003), as well as Tl (Bidoglio et al., 1993). And other studies have suggested that the Fe-Mn colloids can strongly and effectively adsorb ore-forming elements dissolved in seawater, such as Co, Ni, Cu, Zn, Mo, and REE. Ferrihydrite was found to be the most effective scavenger of Mo from seawater (Koschinsky et al., 2003), and REE are adsorbed by Fe-Mn colloids (Bau et al., 1996; Jiang et al., 2011).

Many interface reactions, such as surface adsorption, redox reactions, and surface ectopic catalytic reactions, occur between Fe-Mn minerals and seawater (Hochella, 1990; Stumm, 1992). Surface adsorption and complexation, as well as redox reactions, are the main mechanism through which Fe-Mn minerals accumulate metal cations. Previous studies have mainly discussed the degree of enrichment of various metal elements using phase separation and sequential leaching experiments, and enrichment models of surface adsorption and complexation have been established (Koschinsky and Halbach, 1995; Koschinsky and Hein, 2003; Jiang et al., 2011). However, the original interface of the metallogenic processes in the interface of Fe-Mn minerals and seawater should be considered to determine the enrichment mechanism of ore-forming elements in ferromanganese crusts and nodules as aquatic minerals. The geochemical properties of the mineral surface are closely related to the mineral type, crystal structure, surface structure, and micromorphology. Trace elements exist in seawater systems as dissolved ions, inorganic complexes, and organic coordination polymers. The geochemical behavior of the trace elements is controlled by the reactions of a variety of solutes on the solid particle surface. Therefore, this article focuses on the systematic analysis of the mineralogy and interface effects between Fe-Mn minerals and seawater using X-ray diffraction (XRD), Raman spectroscopy (RS), Fourier transform infrared spectroscopy (FTIR), and X-ray photoelectron spectroscopy (XPS). The crystal structure and surface chemical properties of the Fe-Mn minerals were analyzed and discussed to reveal the relationship between Fe-Mn minerals and the seawater interface and the enrichment mechanism of the ore-forming elements.

2 Experiments

2.1 *Samples*

The samples studied in this paper were dredged from regional surveys of the Zhongjian Islands, Zhongsha Islands, Huangyan Islands and Shantou areas in the South China Sea in 2011 and 2012 by R/V *Haiyangsihao* of the Guangzhou Marine Geological Survey (Fig. 1 and Table 1). Sampling depths ranged from 800 m to

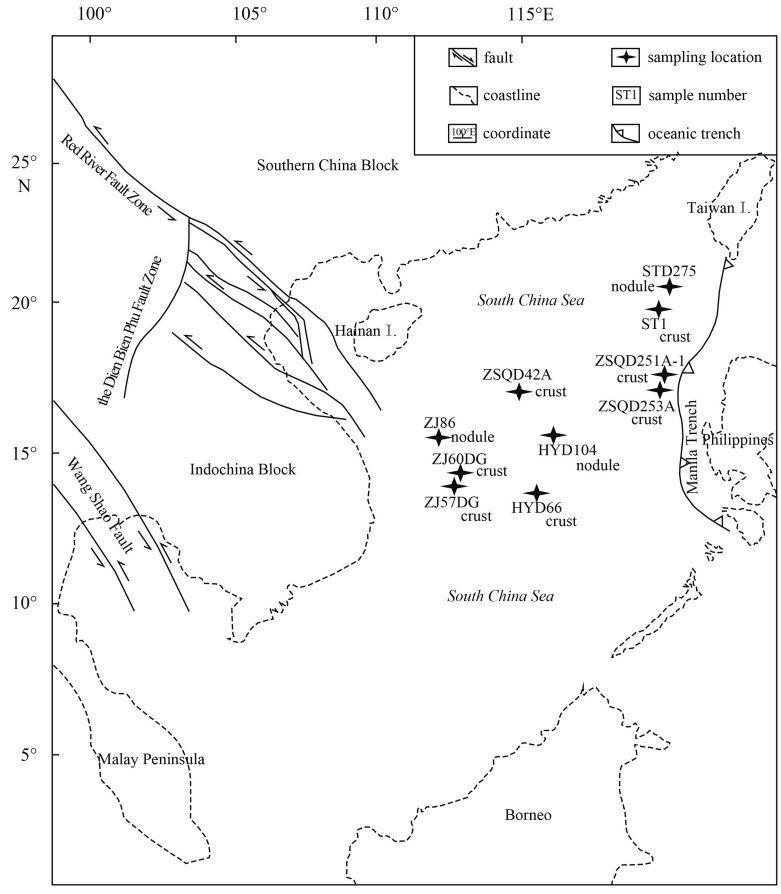

Fig. 1. Sample localities in the South China Sea.

Table 1. Information of polymetallic crusts and nodules from the South China Sea

Sample number	Station number	Sampling location	Coordinate		Depth/m	Feature	XRD mineral composition
ZJ60DG	ZJ60DG	Zhongjian Islands	13°58.388 5′N	113°10.238′E	1 600	crust, dark brown, rough surface, has warty and cauliflower-like protrusions with substrate of carbonate	quartz and vernadite (δ-MnO_2)
ZJ57DG	ZJ57DG	Zhongjian Islands	13°20.175 2′N	113°03.225′E	2 237	crust, dark brown, rough surface, has warty and cauliflower-like protrusions with substrate of carbonate	quartz, vernadite (δ-MnO_2) and plagioclase
ZJ86	ZJ86	Zhongjian Islands	15°20.527 5′N	112°31.467 9′E	1 945	nodule, dark brown, spherical and irregular structure and smooth surface	quartz, vernadite (δ-MnO_2), todorokite and plagioclase
STD275	STD275	Shantou Area	21°41.490 2′N	118°16.745 9′E	1 548	nodule, brown black, the living body shape, ellipsoidal and spherical structure and smooth surface	quartz, vernadite (δ-MnO_2), todorokite and plagioclase
ST1	ST1	Shantou Area	20°28.267′N 20°28.392′N	117°54.375′E 117°54.364′E	1 600	crust, brown black, smooth surface with groove and longitudinal with parallel laminae	quartz, vernadite (δ-MnO_2) and plagioclase
ZSQD42A	ZSQD42A	Zhongsha Islands	16°50.958 6′N	114°49.029 9′E	1 230	crust, dark brown, rough surface with substrate of limestone	quartz and vernadite (δ-MnO_2)
ZSQD251A-1	ZSQD251A-1	Zhongsha Islands	17°13.108 8′N	118°50.866 6′E	1 950	crust, the top surface is smooth and rough side with strumae, with substrate of altered basalt	quartz, vernadite (δ-MnO_2) and plagioclase
ZSQD253A	ZSQD253A	Zhongsha Islands	16°45.986 7′N	118°36.365 9′E	1 150	crust, rough surface with strumae	quartz, vernadite (δ-MnO_2) and plagioclase
HYD66-1	HYD66	Huangyan Islands	13°40.730 7′N	115°16.372 9′E	1 378	crust, dark brown, rough surface with projections, with substrate of altered basalt	quartz, vernadite (δ-MnO_2) and plagioclase
HYD66-2						crust, dark brown, rough surface without projections, with substrate of altered basalt	quartz and vernadite (δ-MnO_2)
HYD104	HYD104	Huangyan Islands	15°33.807 4′N	116°10.908 0′E	815	nodule, dark brown, psephitic structure and rough surface with tubercles	quartz, vernadite (δ-MnO_2), todorokite and plagioclase

2 300 m. All Fe-Mn layers presented as single layers, and the samples were classified as ferromanganese crusts and ferromanganese nodules based on their morphological structures and sedimentary environments. Two seamount ferromanganese crusts from the West Pacific Ocean were also examined for comparison to enhance the analytical results of this study. The two Pacific seamount crusts were obtained from the DY105-13 voyage survey by R/V *Haiyangsihao*. The Fe-Mn minerals of the crusts and nodules were directly analyzed.

2.2 *Instruments and parameters*

XRD: Mineralogical compositions were determined by XRD. This analysis, along with other spectroscopic techniques, was conducted at the Instrumental Analysis and Research Center in Sun Yat-sen University. Bulk XRD analyses were conducted at 40 kV and 150 mA to record diffraction patterns at 2θ ranging from 3° to 90°. The divergence and scattering slits were both 1°, and the receiving slit was 0.3 mm. The step length was 0.02°, and X-ray wavelength λ was 1.541 78 Å. XRD with Ni-filtered CuKα radiation was conducted at a scan speed of 3°/min (2θ).

RS: Raman spectral analysis was performed using a microscopic confocal Raman spectrometer. The clear surfaces of the samples were directly analyzed, and Renishaw InVia was used to record the Raman spectra. The spectrum excitation wavelength was 785 nm, and the best spectral resolution was 1 cm^{-1}. The scanning range was from 50 cm^{-1} to 2 000 cm^{-1}.

FTIR: The KBr powder tablet samples were tested, using a Nicolet6700 Contiuμm (Thermo Scientific). Wave numbers ranged from 4 000 cm^{-1} to 400 cm^{-1}, and the spectral resolution was better than 0.09 cm^{-1}. A DTGS detector and a KBr beam splitter were used.

XPS: X-ray photoelectron spectra were recorded using an ESCALAB 250 system (Thermo Fisher Scientific). The vacuum worked at -2×10^{-9} mbar (under the condition of an open X-ray source), and the X-ray source of monochromatic Al Kα had energies of 1 486.6 eV, 15 kV, and 150 W. The beam spot size was 500 μm, and the scanning mode was CAE. The lens mode was large area XL. Qualitative and quantitative analyses were performed using the Wagner (Al target) Library. Full spectrum scanning was conducted with energy of 100 eV and energy step size of 1 eV/step. Narrow spectrum scanning was conducted with an energy of 20 eV and energy step size of 0.05 eV/step. C1s (284.8 eV) was used as the standard for energy correction (energy scale).

3 Results

3.1 *XRD*

XRD results show that the diffraction curves of the SCS polymetallic crusts and nodules were consistent (Fig. 2). The minerals of the SCS polymetallic crusts were composed of vernadite (δ-MnO_2), quartz, and feldspar, while the polymetallic nodules contained todorokite, vernadite, quartz, and feldspar. No obvious

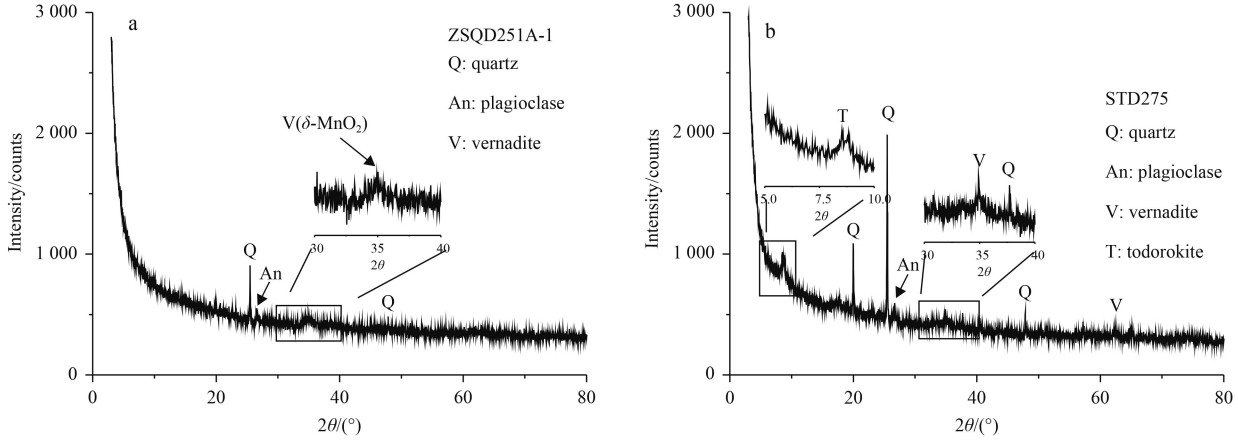

Fig. 2. X-ray diffraction patterns of polymetallic crust and nodule from the South China Sea. a. The crust of ZSQD251A-1 and b. the nodule of STD275.

diffraction peaks of clay minerals and Fe-phase minerals were observed, probably because the crystallinity of the Fe oxides/hydroxides (amorphous ferrihydrite) was very poor or these minerals existed in disperse phases (Shi et al., 1995).

3.2 *RS*

Micro RS can nondestructively analyze the molecular compositions, molecular groups, and crystal structures of minerals. The Raman and standard mineral spectra are shown in Fig. 3. Combined with our XRD results and a previous study (Little et al., 2014), the present results show that the peak should correspond to the crystal lattice vibration of the Mn-O bond with a relatively low bond energy. The main mineral phase was close to a disordered hexagonal birnessite, i.e., δ-MnO_2, which is a mineral unit that forms a sheet (layer)-like stack at the edge of the [MnO_6] octahedron. A lattice vacancy exists in every six [MnO_6] octahedrons in layered structure because of the presence of Mn(Ⅲ) in the [MnO_6] octahedron. The negative charge of the entire octahedral layer is due to this lattice vacancy and the charge is compensated by cations and/or protons between layers through electrostatic interactions (Drits et al., 1997). The peak Raman spectral positions of the Fe-phase reference minerals mainly appeared at wave numbers below 500 cm^{-1}. The main peak position of goethite appeared near 386 cm^{-1}. However, no obvious peak was observed in the range from 0 to 500 cm^{-1}, which indicates that the bond strength of Fe-O in the Fe-phase minerals is very weak. Therefore, the degree of crystallization the Fe-phase minerals in the SCS polymetallic crusts and nodules was very poor. The SCS polymetallic crusts and nodules were mainly amorphous Fe oxides/hydroxides.

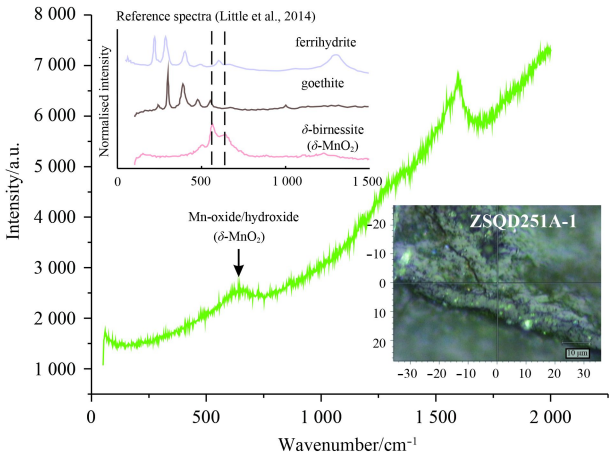

Fig. 3. Raman spectrum of the Fe-Mn mineral of the crust sample ZSQD251A-1 from the South China Sea.

3.3 *FTIR spectroscopy*

The FTIR spectra of the SCS polymetallic crusts and nodules are shown in Figs 4 and 5. The FTIR spectra of the two features were identical and showed minimal differences. Absorption peaks at 3 377–3 388 cm^{-1} indicated -OH stretching vibration. These vibrations could be attributed to free hydroxyl groups and

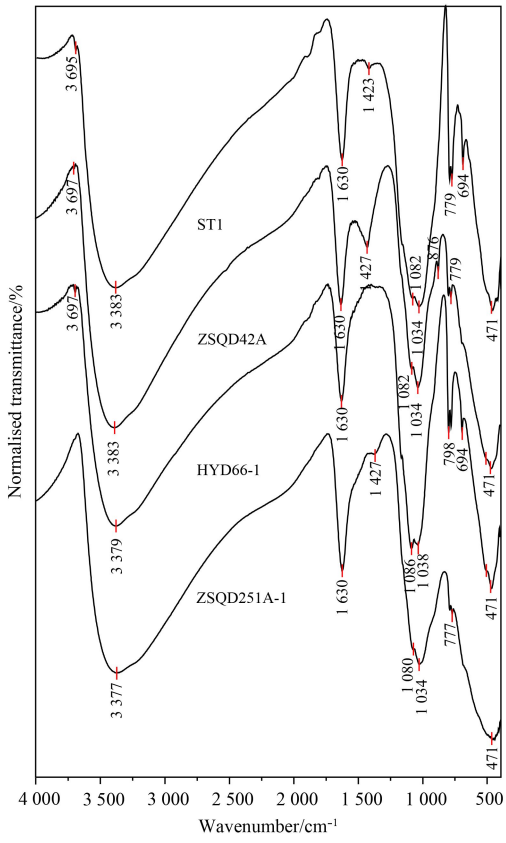

Fig. 4. FTIR spectra of polymetallic crusts from the South China Sea.

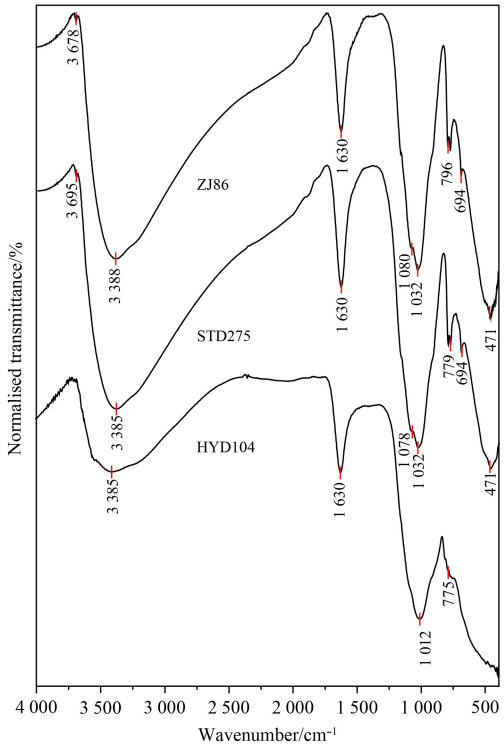

Fig. 5. FTIR spectra of polymetallic nodules from the South China Sea.

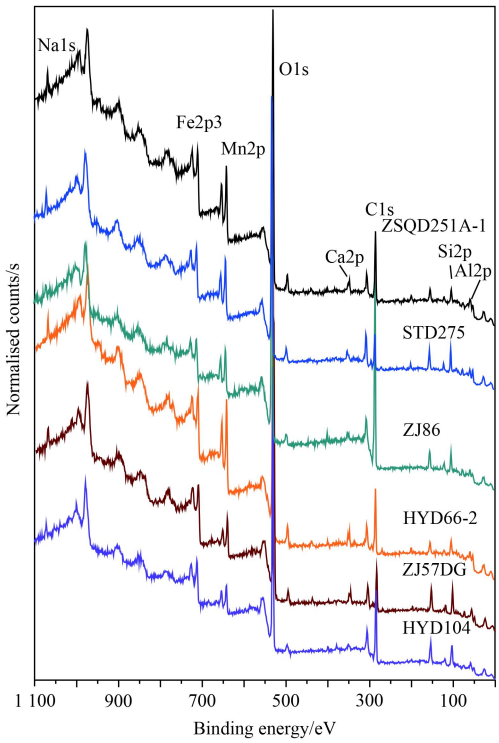

Fig. 6. XPS spectra of polymetallic crusts and nodules from the South China Sea.

hydration of the Fe-Mn mineral surfaces. H-O-H bending vibrations, which are attributed to the adsorptive H_2O molecule (Russell, 1979), were evidenced by a peak at 1 630 cm^{-1}. The vibration absorption peaks of Fe/Mn oxides/hydroxides were different from those of hydrate-hydroxyl groups. The former mainly appeared in the fingerprint zone of the spectra. The absorption peaks of Mn(Ⅲ)-OH vibrations were found in 1 078–1 086 cm^{-1}. The surface hydroxyl (Mn-OH) group of δ-MnO_2 showed peaks at 1 032–1 038 cm^{-1} (Nakamoto, 1978; Liu et al., 2009). The stretching vibrations of Mn-O-Mn, which confirmed the existence of [MnO_6] cell, were evidenced by a peak at 694 cm^{-1} (Naidja et al., 2002). The stretching vibrations of Fe-O-Fe and Fe-OH were evidenced as peaks at 471 cm^{-1} and 775–798 cm^{-1}, respectively (Singh et al., 2000). However, the peak of the bending vibrations of the Fe-OH-Fe surface hydroxyl of goethite, i.e., at 890 cm^{-1} (Liao et al., 2006), was not identified in the spectra, probably because of the presence of numerous surface hydrogen bonds (Fe-OH), which weakened the bond strength of Fe-OH-Fe.

3.4 *XPS*

The full X-ray photoelectron spectra of the SCS polymetallic crusts and nodules are shown in Fig. 6. Two seamount crusts from the Western Pacific Ocean were also analyzed for comparison, and the spectra of these crusts are shown in Fig. 7. Table 2 lists the atomic percentage compositions of the main elements of the mineral surfaces. The results revealed that all of the mineral surfaces in the SCS polymetallic crusts and nodules, as well as those of the Pacific seamount crusts, were mainly composed of Fe, Mn, and O. The mineral surfaces of the SCS crusts and nodules had lower Mn contents but much higher Si, Al, and Ca contents than those of the Pacific seamount crusts. Si, Al, and Ca on the mineral surfaces represented detrital mineral components. This characteristic indicates that the SCS polymetallic crusts and

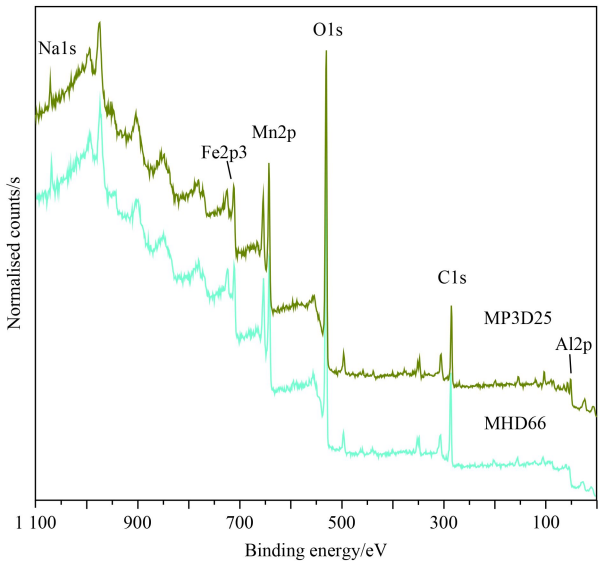

Fig. 7. XPS spectra of the seamount crusts from the Pacific.

nodules were strongly affected by the epicontinental environment, and they exhibited the sedimentary characteristics of marginal sea. Therefore, the fitting spectra of the element narrow spectra for the major elements Fe, Mn, and O on the mineral surfaces were analyzed. Moreover, the chemical valence states and structural patterns of the major elements in the samples were determined.

The O1s spectra of the Fe-Mn mineral surfaces of samples from the South China Sea and Pacific Ocean are shown in Fig. 8. The peak positions of the O1s spectra presented abnormal distributions. The SCS polymetallic crusts and nodules revealed a

Table 2. Main element atomic percentage (At%) of sample surfaces

Location	MHD66 Pacific	MP3D25 Pacific	HYD66-1 South China Sea	HYD66-2 South China Sea	HYD104 South China Sea	STD275 South China Sea	ZJ57DG South China Sea	ZJ86 South China Sea	ZSQD251A-1 South China Sea
Mn2p	9.35	10.26	3.24	7.35	2.97	5.57	3.97	2.86	5.99
Fe2p3	4.74	4.07	2.72	4.58	3.58	4.11	4.45	3.50	8.16
O1s	46.86	50.72	38.66	51.47	47.67	55.04	56.43	39.24	50.09
Si2p	3.03	3.37	4.86	4.53	8.57	7.21	7.37	4.65	4.40
Al2p	0.88	1.46	1.88	2.08	2.33	2.91	2.85	1.86	1.80
Mg1s	2.25	2.14	2.15	2.58	3.15	4.66	3.39	1.79	2.44
Ca2p	1.38	1.29	0.57	1.27	0.78	1.03	1.29	0.78	1.18
Na1s	2.53	2.15	1.55	2.91	2.08	2.73	2.54	1.48	2.36
K2p	–	0.42	0.26	–	0.62	0.71	0.52	–	–
Cl2p	0.94	0.80	0.45	1.00	0.34	0.92	–	–	0.68
Ti2p	0.63	0.57	–	–	–	–	–	–	–
F1s	–	–	0.63	–	0.70	1.26	1.77	–	–
N1s	–	–	1.66	0.94	1.24	0.88	–	–	–
C1s	27.40	22.75	41.38	20.82	25.97	12.96	15.42	43.84	22.88

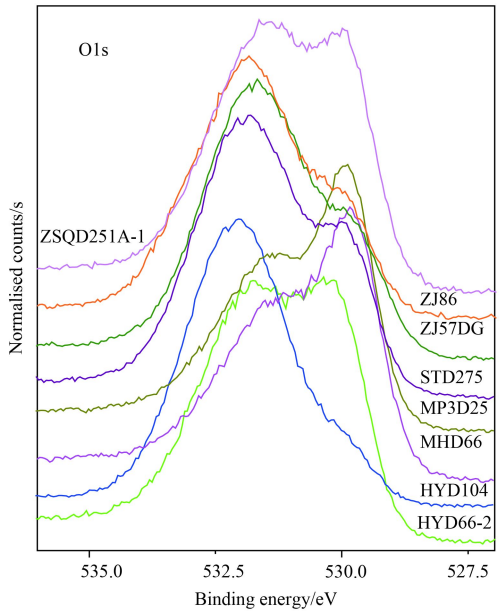

Fig. 8. XPS spectra of O1s of polymetallic crusts and nodules.

sharp main peak in the vicinity of 530.01–532.09 eV with a wide shoulder peak on the right side. Some individual samples demonstrated relatively sharp shoulder peaks. However, the Pacific seamount crusts showed main peaks at around 529.94–529.89 eV with a wide shoulder peak on the left side. These findings suggest that the oxygen exhibited different chemical states on the surfaces of the Fe-Mn minerals, and the main chemical state of surface oxygen in the SCS polymetallic crusts and nodules differed from that of the Pacific Ocean. Previous studies (Knipe et al., 1995; Pratt et al., 1994; Kloprogge et al., 2006) have shown that oxygen has three chemical states namely, lattice oxygen (O^{2-}), hydroxyl (-OH), and hydration oxygen (H_2O). These states correspond to Mn/Fe-O, Mn/Fe-OH, and H-O-H with electron binding energy values of 530, 531, and 533 eV, respectively. The fitting spectra of O1s (Fig. 9) show that the SCS polymetallic crusts and nodules contained a significant amount of hydroxyl (-OH) groups, whereas the Pacific seamount crusts primarily contained lattice oxygen (O^{2-}). This finding indicates that the degree of crystallization of the Fe-Mn minerals of the Pacific seamount crusts was higher than that of minerals from the South China Sea. The hydroxyl (-OH) groups of the mineral surfaces could provide adsorption sites for dissolved metal cations and complex ions in the seawater and release H^+ or hydrated ions during adsorption (Tamura et al., 2001).

The Fe2p spectra of the Fe-Mn mineral surfaces of samples from the South China Sea and Pacific Ocean are shown in Fig. 10. Two obvious peaks of Fe2p were detected at 705–740 eV, including the peak of $Fe2p_{1/2}$ on the left and the peak of $Fe2p_{3/2}$ on the right. The results show that the binding energies and peak strengths of Fe2p of the crusts and nodules surfaces from the South China Sea and the Pacific Ocean are consistent. The binding energy of $Fe2p_{1/2}$ was between 724.9 and 725.6 eV, whereas that of $Fe2p_{3/2}$ was between 711.01 and 712.46 eV. $Fe2p_{1/2}$ and $Fe2p_{3/2}$ had higher binding energies than $Fe2p_{1/2}$ and $Fe2p_{3/2}$ of Fe_2O_3, respectively (Mathieu and Landolt, 1986; Tan et al., 1991). This phenomenon is probably due to the higher binding energy of the Fe and -OH combination than the Fe and O^{2-} combination. This characteristic suggests that Fe exists with a +3 valence in Fe-phase minerals from the South China Sea and Pacific Ocean. Furthermore, according to crystal field energy theory, the occurrence of Fe in a very weak crystal condition implies that the Fe of the mineral phase surfaces mainly combines with the hydroxyl group.

The Mn2p spectra of the Fe-Mn mineral surfaces of samples from the South China Sea and Pacific Ocean are shown in Fig. 11. The binding energy and peak strength of Mn2p of the Fe-Mn mineral surfaces from the South China Sea were similar to those in the Pacific Ocean in the range of 635–660 eV. This result suggests that the chemical states of Mn on the mineral surfaces of the crusts and nodules were consistent. Mn2p was split into a main peak of $Mn2p_{3/2}$ at 642.43–643.06 eV because of spin angular momentum coupling (Fig. 11). The peak of $Mn2p_{1/2}$ was appeared at approximately 654 eV, and the peak shapes of Mn2p showed abnormal distributions. The Mn of the mineral surfaces presents various chemical states. We fit only the peak positions of $Mn2p_{3/2}$ because of the mutually corresponding relationship between $Mn2p_{3/2}$ and $Mn2p_{1/2}$. The fitting spectra are shown in Fig. 12. The peak positions of the standard binding energy of various chemical states of Mn were located at 640.3–641.1, 641.3–641.7, and 641.7–642.2 eV, which corresponded to Mn^{2+}, Mn^{3+}, and Mn^{4+}. Figure 12 shows that the Mn chemical states of the Mn-bearing mineral phases are mainly Mn (IV) and Mn (III).

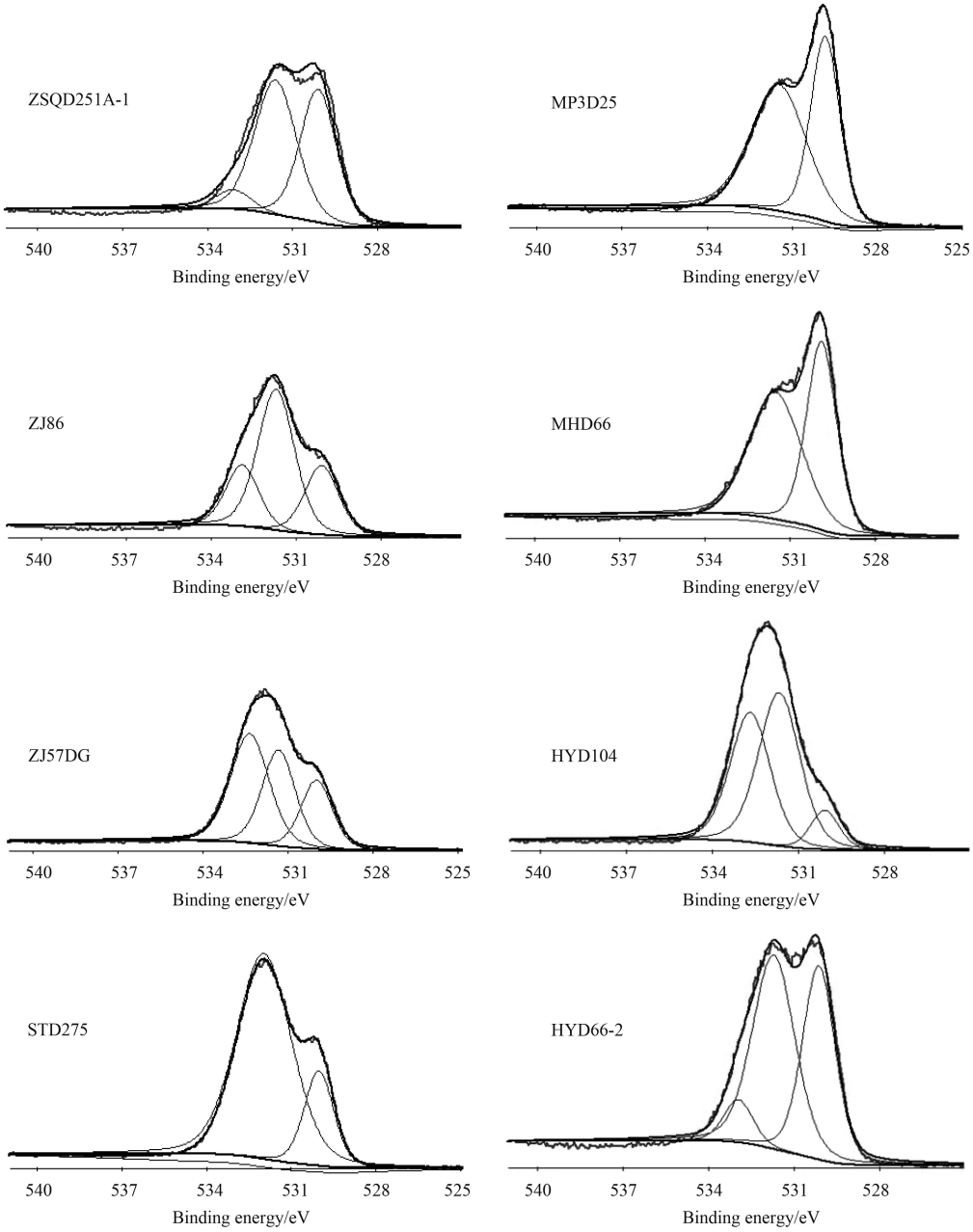

Fig. 9. O1s XPS spectra fitting of polymetallic crusts and nodules.

These results are consistent with the results from synchrotron radiation X-ray generated photo emission electron microscopy (Xue, 2007). Nevertheless, irradiation may cause reductions in the chemical state of Mn during the test process (Garvie and Craven, 1994), but the possibility of the existence of Mn (II) cannot be ruled out. Mn (II) and Mn (III) may exist in the octahedral vacancy and maintain the stability of the mineral crystal structure through electrostatic interactions (Friedrich and Schmitz-Wiechowski, 1980).

4 Discussion

4.1 *Mineral crystallization characteristics*

The XRD results reveal evident diffraction peaks of quartz and feldspar in the SCS polymetallic crusts and nodules. The diffraction peaks of vernadite and todorokite, which are the main Mn-phase minerals, were not sharp, but the peaks were wide and gradual, which indicates that the crystallinities of vernadite and todorokite were relatively poor. Moreover, comparative results of the diffraction curves of the polymetallic crusts and nodules show that the crystallinity of vernadite in the nodules was better than that in the crusts in the South China Sea.

The higher the degree of mineral crystallization, the stronger the bond between elements of groups, and the more likely the Raman spectra will show a peak with small half height-width ratio. Previous studies (Chukhrov et al., 1979; Potter and Rossman, 1979) have indicated that only high-order crystal-structured Mn-phase minerals show evident infrared (IR) spectra characteristics. Mn minerals with different degrees of crystallization show different IR spectral characteristics. This difference can be proven mainly by the quantities of the absorption peak and the ratio of half-peak width and peak height. Therefore, the degree of

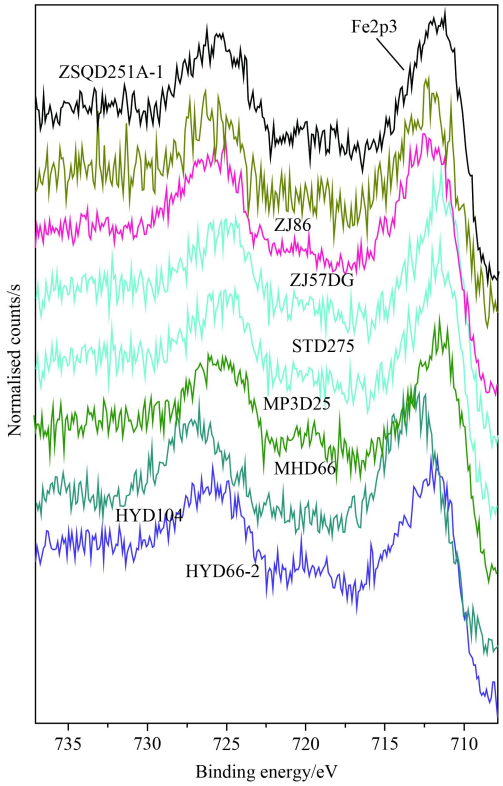

Fig. 10. XPS spectra of Fe2p3 of polymetallic crusts and nodules.

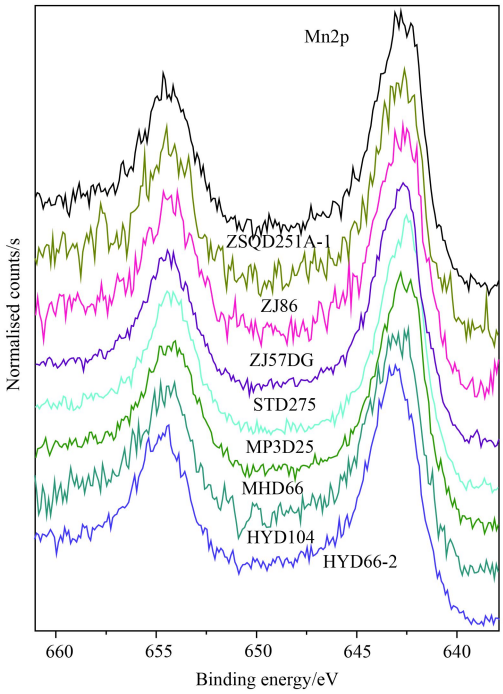

Fig. 11. XPS spectra of Mn2p of polymetallic crusts and nodules.

mineral crystallization of polymetallic crusts and nodules from the South China Sea were very low in the Raman spectra and IR spectra.

The particle size under weak crystallization conditions can strongly influence the surface energy and surface properties of minerals. When the diameter of mineral particles is below 1 nm, the ratio of atomic number of mineral surfaces exceeds 90% (Wang et al., 2003) and nearly all of the atoms are distributed on the surfaces of the nanoparticles. Such a high specific surface area leads to a rapid increase in the atomic number of mineral surfaces and surface energy of minerals. The atomic coordination number of mineral surfaces is insufficient. This phenomenon causes the mineral surfaces to bear very high and unstable chemical activities. The surface atoms of minerals easily bond with other ions (Xue, 2007). Both vernadite and amorphous ferrihydrite have very high specific active surface areas, which are 206 m^2/g for δ-MnO_2 (Yao and Millero, 1996) and approximately 200–300 m^2/g for amorphous ferrihydrite (Dzombak and Morel, 1990). The activity of surface atoms of nanoparticles not only changes the surface atomic configuration of the minerals, but also alters the electron spin conformation and electronic energy spectrum of mineral surfaces (Cao et al., 1999).

Therefore, the presence of amorphous Fe-Mn minerals, which exhibits a pronounced specific surface area and unique nanopores, strengthens the surface energy of these weak crystallization minerals. This characteristic facilitates the occurrence of the interfacial effect between Fe-Mn minerals and seawater.

4.2 *Mineral structure and surface characteristics*

XPS results reveal that the main chemical states of Mn on the Mn-phase mineral surface of the crusts and nodules from the South China Sea and Pacific Ocean were in tetravalent and trivalent states, and may contain a small amount of the divalent state. The crystal chemistry of Mn is influenced by the split of the d orbit in the crystal field, so high-spin state Mn ions present overwhelming superiority. High-spin Mn^{4+}, Mn^{3+}, and Mn^{2+} require crystal field stabilization energies of 12, 6, and 0 dq, respectively, during their octahedral coordination. These ions usually coordinate octahedrally with O^{2-}, OH^-, and H_2O, but Mn^{3+} and Mn^{2+} also present tetrahedron coordination (Xue, 2007). The Mn oxides, which were the main Mn-phase minerals of ferromanganese crusts and nodules, can form surface hydroxylation with water molecules. These hydroxyl sites mainly exist in the forms of Mn-OH^{2+}, Mn-OH, and Mn-O^-, and these forms can reciprocally transform in the following reactions:

$$\begin{aligned} &\text{Mn-OH}^{2+} \rightleftarrows \text{Mn-OH}+\text{H}^+, \\ &\text{Mn-OH} \rightleftarrows \text{Mn-O}^- + \text{H}^+. \end{aligned} \quad (1)$$

The XPS results further show that Fe in the Fe-phase minerals of the crusts and nodules presents in the form of a trivalent ionic bond, similar to that in amorphous goethite and/or lepidocrocite. The surface of goethite exhibits four kinds of surface hydroxyls (Sposito, 1984). Three of these hydroxyl sites are oxo(hydroxo), μ-oxo(μ-hydroxo), and μ3-oxo(μ3-hydroxo), which are named according to the IUPAC rules and structural characteristics. These sites are bonded with 1, 2, and 3 Fe(III) ions, respectively. The fourth hydroxyl site is the Lewis acid, wherein the Fe(III) in the mineral surface shares an electron pair with the -OH in the water molecule. Fe-OH and Fe-OH-Fe in the lattice structure of goethite have their own surface activities because the coordination conditions of the hydroxyl-oxygen vary. The former has a greater hydroxyl chemical activity and higher electronegativity than the latter. Thus, Fe-OH is easier to react with metal cations than Fe-OH-Fe (Xiong and Chen, 1990).

The Fe-Mn minerals of the polymetallic crusts and nodules in the South China Sea are mainly composed of δ-MnO_2, todorokite, and amorphous Fe oxides/hydroxides. The XRD and Raman spectral results confirmed the presence of octahedral [MnO_6]

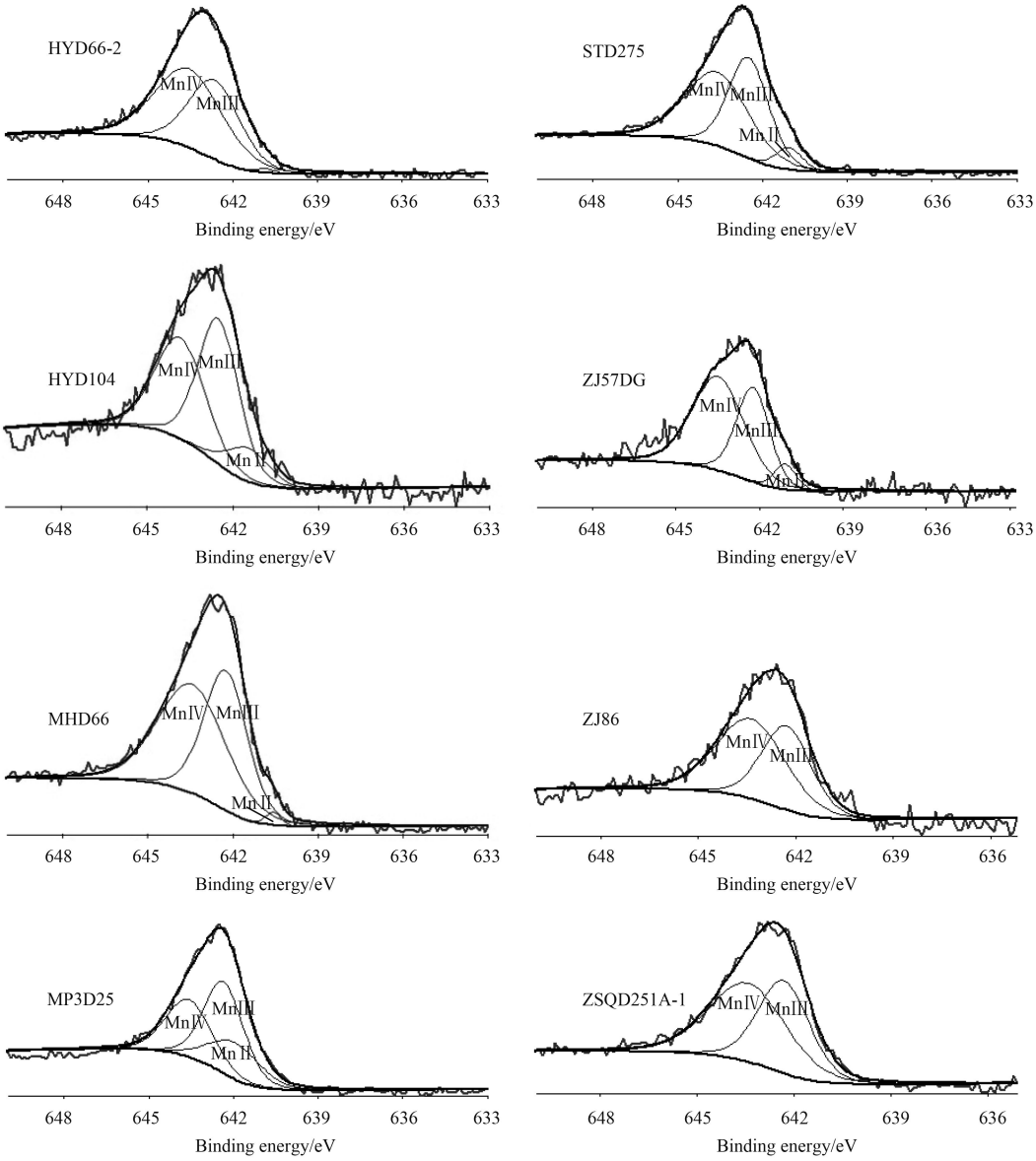

Fig. 12. Mn2p3 XPS spectra fitting of polymetallic crusts and nodules.

unit cell in the Mn phase minerals of the SCS crusts and nodules. The IR spectra further showed the chemical bonds of Mn and Fe on the mineral surfaces with O^{2-} and OH^{-}, respectively. These Fe-Mn minerals belong to the hydroxide mineral group, which presents surface functional groups containing protons. Thus, Fe-Mn minerals could provide an abundant of active sites for complexation of ore-forming elements. The functional groups of mineral surfaces are the basic units of reaction during mineralization complexation.

4.3 *Interface effect and element enrichment*

The surface properties of the SCS polymetallic crusts and nodules were analyzed, and results showed that the surface active sites of the Fe-Mn minerals were the hydroxyl groups. The specific surface area and the nanopore of the Fe-Mn minerals resulted in stronger surface free energy and activity. Moreover, the minerals also increased the bearing capacity and adsorption ability of ions and complex molecules. Many physical and chemical reactions, such as adsorption and exchange of ions, electric potential transfer, and mineral precipitation and solution, occur on mineral surfaces, and the effect of the surface/interface plays the most important role in these reactions. However, the surface effect is closely related to the surface structure and surface groups of minerals. The surface groups of minerals control the chemical activity and reaction mechanism of mineral surfaces (Liu et al., 2001). Therefore, Fe-Mn mineral surfaces could be produced in subsequent complexation reactions between the hydroxyl groups of mineral surfaces and ore-forming elements in seawater.

4.3.1 *Interface inner-sphere complexation*

The functional groups of the mineral surface are the basic units of minerals during participated complexation. Functional groups are the core of surface complexation theory. These groups not only affect the free energy of the complexation reactions between the dissolved state and surface functional groups but also control the chemical measurement of the adsorption reaction and adsorption as well as changes in solution chemical properties (Wei and Wu, 2000). The mineral surface reaction refers to the reaction of mineral surface groups. The types and

properties of surface groups vary according to the types of minerals present. A mineral with different crystal surfaces may have diverse surface group properties. The Fe-Mn minerals of the SCS polymetallic crusts and nodules are composed of δ-MnO_2, amorphous Fe oxides/hydroxides (goethite, lepidocrocite), and todorokite (nodules content). These Fe-Mn minerals are hydroxide minerals, which have surface functional groups containing protons. Surface hydroxyls are the main complexation site. Various types of hydroxyl groups are found on the mineral surface, and different surface hydroxyl groups have distinct reactivities (Davis and Kent, 1990; Hiemstra et al., 1989a, b). Of these, the oxo(hydroxo) site is the most active, and can easily interact with metal cations and complexes in the surface reactions of goethite. Thus, the oxo(hydroxo) site could be highly effective for complexation enrichment of metal cations in seawater. When the surface hydroxy (-O^-) of the Fe-Mn minerals directly bonds with metal cations or complexes in seawater to generate specific adsorption, the enrichment mechanism of ore-forming elements is inner-sphere complexation (Fig. 13a), which bonds with the inner orbit. The reaction of inner-sphere complexes is as follows:

$$M_{Fe\text{-}Mn}\text{-}OH + Me(OH)_x^- \rightarrow M_{Fe\text{-}Mn}\text{-}O\text{-}Me(OH)_{x-1}^- + H_2O. \quad (2)$$

For instance, similar to some highly charged ions, such as Sb^{5+}, and easily hydrolyzed elements, such as Ti and Th, incorporation of Zr, Hf, Nb, and Ta are suggested to occur by the initial formation of inner-sphere surface complexes, followed by surface precipitation of specific hydroxide compounds as solid solutions with the original solid (Farley et al., 1985; Mitsunobu et al., 2006), as well as some transition elements, such as Cu^{2+} (Motschi, 1987). W species can form inner-shpere complexes with the hexavalent state on the ferrihydrite and Mn oxides (Kashiwabara et al., 2013).

4.3.2 *Interface outer-sphere complexation*

Various types of metal cations and complexes in seawater have distinct chemical properties, so Fe-Mn (hydro)oxides have adsorption characteristics and complexation mechanism that may differ from those of other ions and particles. Some metal cations with great hydrated ionic radii generate nonspecific adsorption during uptake onto the surfaces of the Fe-Mn (hydro)oxides (Feng, 2004). Another enrichment mechanism of ore-forming elements in the interface of Fe-Mn minerals and seawater is outer-sphere complexation (Fig. 13b), through which adsorption occurs by the electronegativity of the outer unoccupied orbital ligand.

The Mn and Fe oxides in seawater can form hydrated ions with large surface electrostatic adsorption capacity. The surface energy (charged surface) of Fe-Mn minerals is caused by the adsorption and desorption of H^+ and OH^- ions from mineral surface groups such as -O, -OH, and -OH_2. The charged surface of the Fe-Mn oxides/hydroxides in seawater can form an electric double layer by interacting with diverse charged ions. The surface hydroxyl groups of oxides under certain pH conditions can ionize and function as Bronsted and Lewis acids. The acidity of these groups depends on the distance of the surface hydroxyl groups from the central Fe/Mn ions and is influenced by the strength of the interface electrostatic field (Xue, 2007). Previous studies have shown that the pH_{pzc} (pzc means the point of zero charge) of Mn oxides is 2–4 (Tonkin et al., 2004). The pH_{pzc} of deep-sea manganese nodules is 4.5 (Parida and Mohanty, 1998), while that of vernadite in the crusts is 2.8 (Stumm and Morgan, 1996). By contrast, the pH_{pzc} of amorphous Fe hydroxide [$Fe(OH)_3$] is 8.5 (Stumm, 1992). Therefore, Mn oxides have a negative charge, and amorphous Fe hydroxides have a weak positive charge in seawater (pH 8.0). When the surface charge of the Fe/Mn oxides/hydroxides is neutralized because of adsorption of charged ions, electrostatic repulsion among the particles of mineral surfaces disappears and the particles condense to form outer-sphere complexes. Positively charged species, such as free cations (e.g., Ni^{2+}, Co^{2+}, Zn^{2+}, and Pb^{2+}), and complexes, such as YCO^{3+} and $LREE(OH)^{2+}$, are electrostatically attracted by strongly negatively charged Mn oxide phases. By contrast, negatively charged species of AsO_4^{3-}, PO_4^{3-}, MoO_4^{2-}, and $HREE(CO_3)^{2-}$, as well as uncharged /neutral complexes, such as $SiO_2 \cdot nH_2O$, $Al(OH)\cdot H_2O$, and $Ti(OH)_4^0$, tend to bind to slightly positively charged FeOOH phases (Koschinsky and Halbach, 1995; Koschinsky and Hein, 2003). Mo is a very interesting element. Mo species that could be adsorbed on the surface of ferrihydrite present a tetrahedrally coordinated outer-sphere complex, while that on Mn oxides was an octahedrally coordinated inner-sphere complex (Kashiwabara et al., 2009, 2011).

4.3.3 *Ion exchange*

Similar to zeolite minerals, Mn-phase minerals exhibit molecular sieve effects because of their unique interlayer structure and channel structure. In addition to the two surface complexation models of occupant metal cations at the Fe-Mn mineral surfaces, metal cations occupy the interlayer of water molecules in parallel. These species are primarily alkali metals and alkaline earth metals, such as Mg^{2+}, Ca^{2+}, Ba^{2+}, Na^+, and K^+ (Fig. 13c; Golden et al., 1987; Mellin and Lei, 1993; Feng et al., 1995, 1999). Metal cations, such as Zn^{2+}, Cu^{2+}, and Ni^{2+}, occupy [MnO_6] octahedron vacancies (Feng et al., 1999). Many redox-sensitive metals, such as Co and Ce, can participate in redox reactions at the mineral surfaces during uptake onto Fe-Mn oxide/hydroxide minerals. Moffett and Ho (1996) found that Co presents a positive correlation with Mn in seawater. XANES and XPEEM analytical results indicated that Co has a valence of +3 in natural Mn oxides (Manceau et al., 1992; Xue, 2007). XPS results also showed that Co^{3+} is present in the surface of birnessite, which adsorbs Co^{2+} (Burns, 1976). The adsorptive Co^{2+} may be oxidized to Co^{3+} by Mn^{3+} in the crystal lattices of Mn minerals (Murray and Dillard, 1979; Manceau and Charlet, 1992; Xue, 2007). Therefore, the adsorption and oxidation reactions of Co may mainly occur on the surfaces of Mn oxide minerals. These reactions are the main mechanisms that take place during the concentration of Co into Mn oxide minerals. However, the ionic radius of the Co^{3+} (0.63 Å) is very close to that of Mn^{4+} (0.62 Å), and Co^{3+} can isomorphously substitute the Mn^{4+} in the [MnO_6] octahedron such that Co^{3+} can balance the charge and stabilize the resultant structure (Burns, 1976; Fig. 13c). Therefore, ion exchange of Co^{3+} and Mn^{4+} is one pathway of uptake onto the Mn mineral phase.

5 Conclusions

Many interface reactions, such as surface adsorption, redox reaction, and surface ectopic catalytic reaction, occur between Fe-Mn minerals and seawater (Hochella, 1990; Stumm, 1992). The surface reactions of minerals can be further divided into surface adsorption and complexation, ion exchange, surface eutectic, redox reaction, and catalytic reaction. According to the reaction model, Fe-Mn mineral surfaces possess numerous active sites of hydroxyl groups with protons, because of the unique interlayer and nanopore structure of these minerals in the crusts and nodules. Thus, surface adsorption and complexation, as well

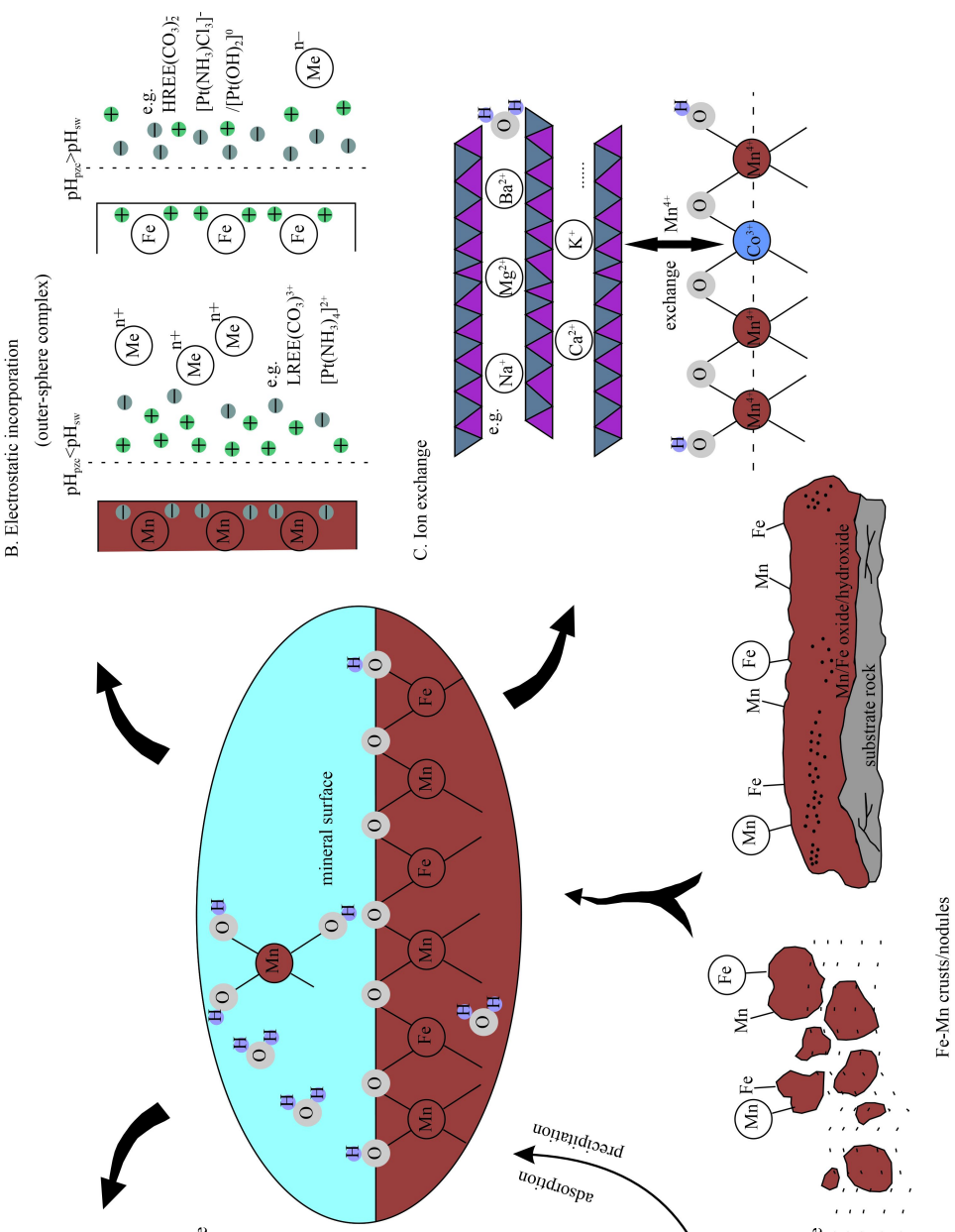

Fig. 13. Model of the interface effect between ferromanganese mineral and seawater. Definition of possible sorption complexes at the mineral/seawater interface, which is represented by the horizontal line. The mineral is below the line and the seawater is above the line. The circles labeled Me represent sorbed metal atoms in various types of sorption complexes. The Me spheres in the mineral and surrounding the metal in seawater are oxygens. The Mn/Fe spheres in the mineral are manganese/iron ions, as are the spheres labeled Me in the sorption complexes and surface precipitate. Modified by Stumm (1992).

as redox reactions are the main pathways by which minerals accumulate metal cations. Therefore, the ore-forming elements in the interface of seawater and the Fe-Mn minerals in the submarine ferromanganese crusts and nodules employ the following enrichment mechanisms. First, the metal ion complexes with the surface hydroxyl groups of Fe-Mn minerals to form hydroxyl complexes, which are connected by coordination bonds or stable inner-sphere complexes that exchange protons on the colloid surfaces. Second, the charged surfaces of the minerals and metal cations form outer-sphere complexes, which make up the electrostatic double layer, through electrostatic interaction. Finally, the metal cations isomorphously exchange the Mn and Fe ions of the mineral lattice structure.

Acknowledgements

The authors thank the Guangzhou Marine Geological Survey for supplying the samples and two anonymous reviewers for their professional comments that improved this manuscript.

References

Bau M, Koschinsky A, Dulski P, et al. 1996. Comparison of the partitioning behaviours of yttrium, rare earth elements, and titanium between hydrogenetic marine ferromanganese crusts and seawater. Geochimica et Cosmochimica Acta, 60(10): 1709–1725

Bidoglio G, Gibson P N, O'Gorman M, et al. 1993. X-ray absorption spectroscopy investigation of surface redox transformations of thallium and chromium on colloidal mineral oxides. Geochimica et Cosmochimica Acta, 57(10): 2389–2394

Burns R G. 1976. The uptake of cobalt into ferromanganese nodules, soils, and synthetic manganese (IV) oxides. Geochimica et Cosmochimica Acta, 40(1): 95–102

Cao Lixin, Wan Haibao, Wang Shubin, et al. 1999. The effect of surface structure on the photoluminescence of SnO_2 nanoparticles in hydrosols and organosols. Spectroscopy and Spectral Analysis (in Chinese), 19(5): 651–654

Chukhrov F V, Gorshkov A I, Sivtsov A V, et al. 1979. New data on natural todorokites. Nature, 278(5705): 631–632

Davis J A, Kent D B. 1990. Surface complexation modeling in aqueous geochemistry. In: Hochella Jr M F, White A F, eds. Mineral-water Interface Geochemistry: Reviews in Mineralogy, Volume 23. Washington D C: Mineralogical Society of America, 177–260

Drits V A, Silvester E, Gorshkov A I, et al. 1997. Structure of synthetic monoclinic Na-rich birnessite and hexagonal birnessite: I. results from X-ray diffraction and selected-area electron diffraction. American Mineralogist, 82(9–10): 946–961

Dzombak D A, Morel F M M. 1990. Surface Complexation Modeling: Hydrous Ferric Oxide. New York: Wiley, 81–95

Farley K J, Dzombak D A, Morel F M M. 1985. A surface precipitation model for the sorption of cations on metal oxides. Journal of Colloid and Interface Science, 106(1): 226–242

Feng Qi, Kanoh H, Miyai Y, et al. 1995. Alkali metal ions insertion/extraction reactions with hollandite-type manganese oxide in the aqueous phase. Chemistry of Materials, 7(1): 148–153

Feng Qi, Kanoh H, Ooi K. 1999. Manganese oxide porous crystals. Journal of Materials Chemistry, 9(2): 319–333

Feng Xionghan. 2004. Syntheses, transformations and surface chemistry characteristics of the common manganese oxide minerals in soils (in Chinese) [dissertation]. Wuhan: Huazhong Agricultural University

Friedrich G, Schmitz-Wiechowski A. 1980. Mineralogy and chemistry of a ferromanganese crust from a deep-sea hill, central Pacific, "Valdivia" cruise VA 132. Marine Geology, 37(1–2): 71–90

Garvie L A J, Craven A J. 1994. High-resolution parallel electron energy-loss spectroscopy of Mn $L_{2,3}$-edges in inorganic manganese compounds. Physics and Chemistry of Minerals, 21(4): 191–206

Golden D C, Chen C C, Dixon J B. 1987. Transformation of birnessite to buserite, todorokite, and manganite under mild hydrothermal treatment. Clays and Clay Minerals, 35(4): 271–280

Guan Yao, Sun Xiaoming, Shi Guiyong, et al. 2017. Rare earth elements (REE) composition and constraints on the genesis of the polymetallic crusts and nodules in the South China Sea. Acta Geologica Sinica (English Edition) (in press)

Halbach P, Kriete C, Prause B, et al. 1989. Mechanisms to explain the platinum concentration in ferromanganese seamount crusts. Chemical Geology, 76(1–2): 95–106

He Gaowen, Ma Weilin, Song Chengbing, et al. 2011a. Distribution characteristics of seamount cobalt-rich ferromanganese crusts and the determination of the size of areas for exploration and exploitation. Acta Oceanologica Sinica, 30(3): 63–75

He Gaowen, Sun Xiaoming, Xue Ting. 2011b. A Comparative Study of the Geology, Geochemistry and Metallogenetic Mechanism of Polymetallic Nodules and Cobalt-rich Crusts from the Pacific Ocean (in Chinese). Beijing: Geological Publishing House

Hein J R, Koschinsky A. 2014. Deep-ocean ferromanganese crusts and nodules. In: Holland H D, Turekian K K, eds. Treatise on Geochemistry. 2nd ed. Amsterdam: Elsevier, 273–291

Hein J R, Koschinsky A, Bau M, et al. 2000. Cobalt-rich ferromanganese crusts in the Pacific. In: Cronan D S, ed. Handbook of Marine Mineral Deposits. Boca Raton: CRC Press, 239–279

Hein J R, Koschinsky A, Halliday A N. 2003. Global occurrence of tellurium-rich ferromanganese crusts and a model for the enrichment of tellurium. Geochimica et Cosmochimica Acta, 67(6): 1117–1127

Hein J R, Spinardi F, Okamoto N, et al. 2015. Critical metals in manganese nodules from the Cook Islands EEZ, abundances and distributions. Ore Geology Reviews, 68: 97–116

Hiemstra T, De Wit J C M, Van Riemsdijk W H. 1989a. Multisite proton adsorption modeling at the solid/solution interface of (hydr)oxides: a new approach, 2. Application to various important (hydr)oxides. Journal of Colloid and Interface Science, 133(1): 105–117

Hiemstra T, Van Riemsdijk W H, Bolt G H. 1989b. Multisite proton adsorption modeling at the solid/solution interface of (hydr)oxides: a new approach: I. Model description and evaluation of intrinsic reaction constants. Journal of Colloid and Interface Science, 133(1): 91–104

Hochella Jr M F. 1990. Atomic structure, microtopography, composition, and reactivity of mineral surfaces. In: Hochella Jr M F, White A F, eds. Mineral-water Interface Geochemistry: Reviews in Mineralogy, v 23. Washington D C: Mineralogical Society of America, 87–132

Jiang Xuejun, Lin Xuehui, Yao De, et al. 2011. Enrichment mechanisms of rare earth elements in marine hydrogenic ferromanganese crusts. Science China: Earth Sciences, 54(2): 197–203

Kashiwabara T, Takahashi Y, Marcus M A, et al. 2013. Tungsten species in natural ferromanganese oxides related to its different behavior from molybdenum in oxic ocean. Geochimica et Cosmochimica Acta, 106: 364–378

Kashiwabara T, Takahashi Y, Tanimizu M. 2009. A XAFS study on the mechanism of isotopic fractionation of molybdenum during its adsorption on ferromanganese oxides. Geochemical Journal, 43(6): e31–e36

Kashiwabara T, Takahashi Y, Tanimizu M, et al. 2011. Molecular-scale mechanisms of distribution and isotopic fractionation of molybdenum between seawater and ferromanganese oxides. Geochimica et Cosmochimica Acta, 75(19): 5762–5784

Kloprogge J T, Duong L V, Wood B J, et al. 2006. XPS study of the major minerals in bauxite: gibbsite, bayerite and (pseudo-) boehmite. Journal of Colloid and Interface Science, 296(2): 572–576

Knipe S W, Mycroft J R, Pratt A R, et al. 1995. X-ray photoelectron spectroscopic study of water adsorption on iron sulphide minerals. Geochimica et Cosmochimica Acta, 59(6): 1079–1090

Koschinsky A, Halbach P. 1995. Sequential leaching of marine ferromanganese precipitates: genetic implications. Geochimica et Cosmochimica Acta, 59(24): 5113–5132

Koschinsky A, Hein J R. 2003. Uptake of elements from seawater by

ferromanganese crusts: solid-phase associations and seawater speciation. Marine Geology, 198(3–4): 331–351

Koschinsky A, Winkler A, Fritsche U. 2003. Importance of different types of marine particles for the scavenging of heavy metals in the deep-sea bottom water. Applied Geochemistry, 18(5): 693–710

Kuhn T, Bau M, Blum N, et al. 1998. Origin of negative Ce anomalies in mixed hydrothermal-hydrogenetic Fe-Mn crusts from the Central Indian Ridge. Earth and Planetary Science Letters, 163(1–4): 207–220

Liao Shuijiao, Wang Juan, Zhu Duanwei, et al. 2006. Structural characteristics of goethite and its B-loaded oxides. Acta Pedologica Sinica (in Chinese), 43(5): 742–748

Little S H, Sherman D M, Vance D, et al. 2014. Molecular controls on Cu and Zn isotopic fractionation in Fe-Mn crusts. Earth and Planetary Science Letters, 396: 213–222

Liu Chongxuan, Kota S, Zachara J M, et al. 2001. Kinetic analysis of the bacterial reduction of goethite. Environmental Science & Technology, 35(12): 2482–2490

Liu Ruiping, Liu Huijuan, Qiang Zhimin, et al. 2009. Effects of calcium ions on surface characteristics and adsorptive properties of hydrous manganese dioxide. Journal of Colloid and Interface Science, 331(2): 275–280

Manceau A, Charlet L. 1992. X-ray absorption spectroscopic study of the sorption of Cr(III) at the oxide-water interface: I. Molecular mechanism of Cr(III) oxidation on Mn oxides. Journal of Colloid and Interface Science, 148(2): 425–442

Manceau A, Gorshkov A I, Drits V A. 1992. Structural chemistry of Mn, Fe, Co, and Ni in manganese hydrous oxides: Part II. Information from EXAFS spectroscopy and electron and X-ray diffraction. American Mineralogist, 77: 1144–1157

Mathieu H J, Landolt D. 1986. An investigation of thin oxide films thermally grown *in situ* on Fe-24Cr and Fe-24Cr-11Mo by auger electron spectroscopy and X-ray photoelectron spectroscopy. Corrosion Science, 26(7): 547–559

Mellin T A, Lei Guobin. 1993. Stabilization of 10Å-manganates by interlayer cations and hydrothermal treatment: implications for the mineralogy of marine manganese concretions. Marine Geology, 115(1–2): 67–83

Mitsunobu S, Harada T, Takahashi Y. 2006. Comparison of antimony behavior with that of arsenic under various soil redox conditions. Environmental Science & Technology, 40(23): 7270–7276

Moffett J W, Ho J. 1996. Oxidation of cobalt and manganese in seawater via a common microbially catalyzed pathway. Geochimica et Cosmochimica Acta, 60(18): 3415–3424

Motschi H. 1987. Aspects of the molecular structure in surface complexes: spectroscopic investigations. In: Stumm W, ed. Aquatic Surface Chemistry. New York: John Wiley and Sons, 111–126

Murray J W, Dillard J G. 1979. The oxidation of cobalt(II) adsorbed on manganese dioxide. Geochimica et Cosmochimica Acta, 43(5): 781–788

Naidja A, Liu C, Huang P M. 2002. Formation of protein-birnessite complex: XRD, FTIR, and AFM analysis. Journal of Colloid and Interface Science, 251(1): 46–56

Nakamoto K. 1978. Infrared and Raman Spectra of Inorganic and Coordination Compounds. 3rd ed. New York: John Wiley, 324–330

Parida K M, Mohanty S. 1998. Studies on Indian Ocean manganese nodules: VIII. Adsorption of aqueous phosphate on ferromanganese nodules. Journal of Colloid and Interface Science, 199(1): 22–27

Potter R M, Rossman G R. 1979. The tetravalent manganese oxides: identification, hydration, and structural relationships by infrared spectroscopy. American Mineralogist, 64: 1199–1218

Pratt A R, Muir I J, Nesbitt H W. 1994. X-ray photoelectron and Auger electron spectroscopic studies of pyrrhotite and mechanism of air oxidation. Geochimica et Cosmochimica Acta, 58(2): 827–841

Russell J D. 1979. Infrared spectroscopy of ferrihydrite: evidence for the presence of structural hydroxyl groups. Clay Minerals, 14(2): 109–114

Shi Nicheng, Ma Zhesheng, He Wanzhong, et al. 1995. Nano-solids in manganese nodules from northern part of Pacific Ocean floor-Nano-solids in minerals and prospects of its uses in industry. Science in China Series B: Chemistry, 38(12): 1493–1500

Singh B, Sherman D M, Gilkes R J, et al. 2000. Structural chemistry of Fe, Mn, and Ni in synthetic hematites as determined by extended X-ray absorption fine structure spectroscopy. Clays and Clay Minerals, 48(5): 521–527

Sposito G. 1984. The Surface Chemistry of Soils. New York: Oxford University Press

Stumm W. 1992. Chemistry of the Solid-water Interface: Processes at the Mineral-water and Particle-water Interface in Natural Systems. New York: John Wiley and Sons

Stumm W, Morgan J J. 1996. Aquatic Chemistry. New York: John Wiley and Sons

Tamura H, Mita K, Tanaka A, et al. 2001. Mechanism of hydroxylation of metal oxide surfaces. Journal of Colloid and Interface Science, 243(1): 202–207

Tan B J, Klabunde K J, Sherwood P M A. 1991. XPS studies of solvated metal atom dispersed (SMAD) catalysts. Evidence for layered cobalt-manganese particles on alumina and silica. Journal of the American Chemical Society, 113(3): 855–861

Tonkin J W, Balistrieri L S, Murray J W. 2004. Modeling sorption of divalent metal cations on hydrous manganese oxide using the diffuse double layer model. Applied Geochemistry, 19(1): 29–53

Wang Yifeng, Bryan C, Xu Huifang, et al. 2003. Nanogeochemistry: geochemical reactions and mass transfers in nanopores. Geology, 31(5): 387–390

Wei Junfeng, Wu Daqing. 2000. Surface ionization and surface complexation models at mineral/water interface. Advance in Earth Sciences (in Chinese), 15(1): 90–96

Xiong Yi, Chen Jiafang. 1990. Soil Colloid (Part III): Properties of Soil Colloid (in Chinese). Beijing: Science Press

Xue Ting. 2007. Geochemical characters and ore-forming elements enrichment mechanism of ferromanganese crusts from Pacific Ocean (in Chinese) [dissertation]. Guangzhou: Sun Yat-sen University

Yao Wensheng, Millero F J. 1996. Adsorption of phosphate on manganese dioxide in seawater. Environmental Science & Technology, 30(2): 536–541